Mesh Quality: A Function of Geometry, Error Estimates or Both?

M.Berzins

Computational PDEs Unit, School of Computer Studies, The University, Leeds LS2 9JT. *

Abstract. *The issue of mesh quality for unstructured triangular and tetrahedral meshes is considered. The theoretical background to finite element methods is used to understand the basis of present-day geometrical mesh quality indicators. A survey of more recent research in the development of finite element methods reveals work on anisotropic meshing algorithms and on providing good error estimates that reveal the relationship between the error and both the mesh and the solution gradients. The reality of solving complex three dimensional problems is that such indicators are presently not available for many problems of interest. A simple tetrahedral mesh quality measure using both geometrical and solution information is described. Some of the issues in mesh quality for unstructured tetrahedral meshes are illustrated by means of two simple examples.*

Keywords. Mesh quality, unstructured meshes, error estimates, mesh generation.

1 Introduction

The range of partial differential equations problems (p.d.e.s) solved by finite element and finite volume solvers based on triangular and tetrahedral meshes e.g [1] [2] is rapidly increasing. The original applications problem class for many such solvers was in the area of solid mechanics and elasticity in particular. These methods are being applied at present to a wide range of problems in solid and fluid mechanics ranging from linear elasticity to turbulent flows, [3, 4]. This very broad spectrum of applications naturally raises the issue of whether or not the meshes being used are appropriate for the applications being considered. This issue of what is an appropriate mesh is as old as the finite element method itself, but the increasingly complex nature of 3D applications may involve dealing with multicomponent problems with time dependence, turbulence and anisotropy to name but some of many possible complications.

A relatively simple example which is useful to illustrate the difficulties is the following 3D advection reaction problem, which is taken from a model of atmospheric dispersion from a power station plume - a concentrated source of NOx emissions, [5]. The photochemical reaction of this NOx with polluted air leads to the generation of ozone at large distances downwind from the source. An accurate description of the distribution of pollutant concentrations is needed over large spatial regions in order to compare with field measurement calculations. The present trend is to use models incorporating an ever larger number of reactions and chemical species in the atmospheric chemistry model. The complex chemical kinetics in the atmospheric model gives rise to abrupt and sudden changes in the concentration of the chemical species in both space and time. These changes must be matched by changes in the spatial mesh and the timesteps if high resolution is required, [5]. This application is modelled by the atmospheric diffusion equation in three space dimensions given by:

$$\frac{\partial c_s}{\partial t}+\frac{\partial u c_s}{\partial x}+\frac{\partial v c_s}{\partial y}+\frac{\partial w c_s}{\partial z}=D+R_s+E_s-\kappa_s c_s, \quad (1)$$

where c_s is the concentration of the s'th compound, u,v and w, are wind velocities and κ_s is the sum of the wet and dry deposition velocities. E_s describes the distribution of emission sources for s'th compound and R_s is the chemical reaction term which may contain nonlinear terms in c_s. D is the diffusion term set to zero here. For n chemical species an set of n partial differential equations (p.d.e's) is formed where each is coupled to the others through the nonlinear chemical reaction terms.

The test case model is based on that used by [5] and covers a region of 300 x 500 km. The chemical mechanism contains only 7 species but still represents the main features of a tropospheric mechanism, namely the competition of the fast inorganic reactions, [5], with the chemistry of volatile organic compounds

* *Correspondence and offprint requests to:* Dr M.Berzins Computational PDEs Unit, School of Computer Studies, The University, Leeds LS2 9JT. Email: martin@scs.leeds.ac.uk

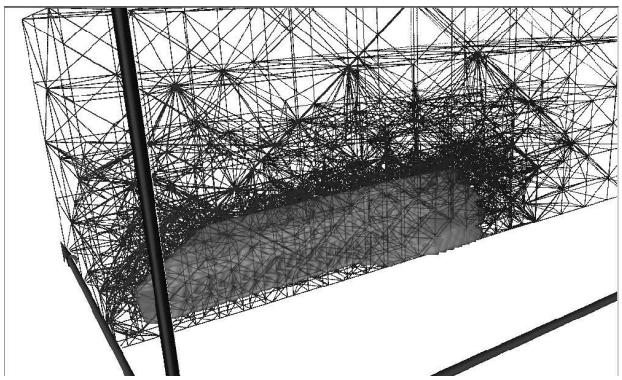

Figure 1: Tetrahedral Mesh for Reacting Flow P.D.E.

(VOC's), which occurs on a much slower time-scale. The power station is taken to be the only source of NOx and hence the initial grid will contain more elements close to this concentrated emission source.

Figure 1 shows the plume developing with the adaptive mesh clustered around the developed portion of the solution. The visualisation was realised by running the parallel code in conjunction with the SCIRUN system at the University of Utah, see [6]. The main area of mesh refinement is along the plume edges close to the chimney. Using the adaptive mesh, we can clearly see the plume edges and can easily identify areas of high concentrations. The effects of the plume on ozone concentrations also provides some interesting results. Close to the plume the concentration of O_3 is much lower than that in the background. Due to the high NOx concentrations the inorganic chemistry is dominant in this region and ozone is consumed. As the plume travels downwind and the NOx levels decrease, the plume gradually picks up emissions of VOC's and leads to the production of NO_2 which in turn causes levels of ozone to rise above the background levels at quite large distances downwind from the source of NOx.

The issue of whether the mesh is appropriate for this application is somewhat more complex than for a simple linear problem. Strong local variations in solution component values make it difficult to assess the quality of the mesh for each component without somehow incorporating solution behaviour.

1.1 Background Results

In order to start to understand the issue of mesh quality it is important to review the important finite element results that formed a basis for existing mesh quality measures. In order to state these results it is necessary to introduce some notation. Without loss of generality the case of linear finite elements on triangular or tetrahedral meshes will be considered. Define the error as being the difference between the linear approximation, u_{lin} and the true solution u i.e. $e_{lin}(x,y) = u_{lin}(x,y) - u(x,y)$. The L^2 error norm is defined by $||e_{lin}(x,y)||_{L^2}$ where

$$||e_{lin}(x,y)||^2_{L^2} = \int_T (e_{lin}(x,y))^2 dxdy \ . \qquad (2)$$

The H^1 error norm is defined by $||e_{lin}(x,y)||_{H^1}$ where

$$||e_{lin}(x,y)||^2_{H^1} = \int_T (e_{lin}(x,y))^2 + (e_{lin,x}(x,y))^2 + (e_{lin,y}(x,y))^2 dxdy \ . \qquad (3)$$

The seminorm of the H^2 space is defined by $|u|_2$ where

$$|u|_2 = \left(\sum_{|\delta|=2} \frac{2!}{\delta_1! \delta_2!} ||(\partial_x)^{\delta_1} (\partial_y)^{\delta_2} u||^2_{L^2} \right)^{1/2} . \qquad (4)$$

Aside from the notion that meshes with regular or smoothly varying element sizes are more aesthetically pleasing, the starting point for the notion of mesh quality would appear to be the analysis leading to the minimum angle condition that the smallest angle should be bounded away from zero. This perhaps originated with Zlamal [7] and is quoted by Strang and Fix [8] together with a statement regarding how *poorly shaped* triangles may have an effect on the condition number of the linear algebra problem that must be solved. This result was improved by Babuska and Aziz [9], who showed that the correct requirement for triangles was that there should be no large angles. The general results of both Zlamal and Babuska and Aziz are of the form

$$||e_{lin}(x,y)||^2_{H^1} \ \leq \ \Gamma(\theta)|u|_2 \qquad (5)$$

where Zlamal [7] showed that $\Gamma(\theta) = h/sin(\theta_{min})$ for the minimum angle $\theta_{min} = min(\theta_1, \theta_2, \theta_3)$, see Figure 2. In improving this result Babuska and Aziz [9] showed that $\Gamma(\theta) = h/\Psi(\theta)$ where $\Psi(\theta)$ is a positive continuous and finite function and for $\theta \leq \gamma < \pi, \Psi(\theta) \geq \Psi(\gamma)$ where γ is a bound on the maximum interior angle of the triangle in Figure 2. Many other similar results were proved at around the same time. The comprehensive Habilitationschrift thesis of Appel [10] contains a unified theory of interpolation error estimates and also describes and references these

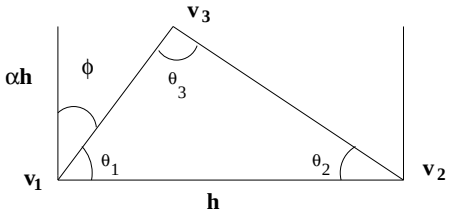

Figure 2: Babuska and Aziz Example Triangle.

results. Appel's work also extends to tetrahedra and includes a discussion of the work of Krizek [11] and others which extends the work of Babuska and Aziz to three dimensions.

Anecdotal evidence confirms that these results influenced mesh generation code writers. Early mesh generation papers are covered by the surveys of Shephard [12] and Thacker [13]. In these surveys there is little explicit reference to how the theoretical work has been adopted, though Thacker does say that elements should be nearly equilateral otherwise instability may result. More recent surveys by Bern and Epstein [14] and Nielson [15], do mention the theoretical results and the monographs of Carey [16] and George and Borouchaki [17] treat the subject in more detail. The perceived meshing wisdom has thus been that if possible elements should have no small or large angles. In the case of tetrahedral meshes this has has led to geometric mesh quality indicators as described in Liu and Joe [18], one example being Weatherill's edge quality estimator [2] for tetrahedra of volume V and edge lengths h_i:

$$Q_w = \frac{1}{8.48528V} \left[(\Sigma \frac{h_i}{6})^3 \right]. \qquad (6)$$

Such indicators do a good job of identifying geometric imperfections in the mesh -an important task before any solution is computed on the mesh. The difficulty is that it is unclear that such indicators are valid for every solution on every mesh. The ideal solution is thus to understand the relationship between the error and the mesh. Recently there have been many attempts to dynamically modify triangular meshes so as to fit the solution better. Some of these approaches will be described below - most of them lead to stretched meshes for anisotropic solutions. The main requirement is thus for error estimators that include both solution and geometry information. Such estimators are still in their infancy especially in 3D but it will be shown that it is possible to use interpolation errors, [19] and, through simple examples on tetrahedral meshes, that the accuracy in the solution can depend critically on the mesh.

2 A Finite Element Theory Based Quality Indicator

The decision as to whether or not (and how) a mesh should be refined should be based on an error estimate that reflects not only the interpolation error caused by approximating the solution by a finite element space on a given mesh but also the discretization error of the numerical method used to approximate the p.d.e. and the choice of norm used to measure the error. Rippa [20] makes a convincing case based on interpolation errors that long thin triangles do indeed form part of a good mesh for strongly anisotropic solutions. A good discussion of this topic also occurs in Nielson [15] and a very precise and complete mathematical analysis in Appel [10].

Berzins [19] derives a new mesh quality indicator from the work of Nadler [21] which gives a particularly appropriate expression for the interpolation error when a quadratic function is approximated by a piecewise linear function on a triangle. Consider the triangle T defined by the vertices v_1, v_2 and v_3 as shown in Figure 2. Let h_i be the length of the edge connecting v_i and v_{i+1} where $v_4 = v_1$. Nadler [21] considers the case in which a quadratic function

$$u(x,y) \;=\; \frac{1}{2}\underline{x}^T \; H \; \underline{x} \; where \quad \underline{x} \;=\; [x,y]^T, \qquad (7)$$

where H is a constant 2×2 real matrix, which is also the Hessian matrix, is approximated by a linear function $u_{lin}(x,y)$, as defined by linear interpolation based on the values of u at the vertices and shows that the error denoted by equation (2) above satisfies

$$\int_T (e_{lin}(x,y))^2 dx \; dy \;=$$
$$\frac{A}{180}\left[((d_1+d_2+d_3)^2 + {d_1}^2 + d_2^2 + d_3^3\right] \qquad (8)$$

where A is the area of the triangle and $d_i = \frac{1}{2}(v_{i+1} - v_i)^T \; H \; (v_{i+1} - v_i)$ is the edge derivative along the v_i and v_{i+1} edge. Berzins [14] uses this result as the basis for an indicator that takes into account both the geometry and the solution behaviour by defining scaled edge derivatives by $\tilde{d}_i = |d_i|/d_{max}$ where $d_{max} \;=\; max\,[|d_1|, |d_2|, |d_3|]$. For notational convenience define $\underline{\tilde{d}} = [\tilde{d}_1, \tilde{d}_2, \tilde{d}_3]^T$ and

$$\tilde{q}(\underline{\tilde{d}}) \;=\; (\tilde{d}_1 + \tilde{d}_2 + \tilde{d}_3)^2 + \tilde{d}_1^2 + \tilde{d}_2^2 + \tilde{d}_3^2 \qquad (9)$$

A measure of the anisotropy in the derivative contributions to the error is then provided by

$$q_{aniso} \;=\; \tilde{q}(\underline{\tilde{d}})/12. \tag{10}$$

The relationship between q_{aniso} and the linear interpolation error is that in the case when the matrix H is positive definite, i.e. $d_i > 0$, then the indicator q_{aniso} is a scaled form of the interpolation error, [19], in this special case.

A consistent and related but geometry-only based indicator is then defined by:

$$q_m(\underline{h}) = \tilde{q}(\underline{h})/(16\ \sqrt{3}\ A), \tag{11}$$

where $\underline{h} = [h_1, h_2, h_3]^T$, has value 1 for an equilateral triangle and tends to the value infinity as the area of a triangle tends to zero but at least one of its sides is constant. Bank [1] and Weatherill's [2] indicators are denoted by q_b and q_w and defined by

$$\begin{aligned} \frac{1}{q_b} \;&=\; \frac{1}{4\ \sqrt{3}\ A}\left[(h_1^2 + h_2^2 + h_3^2\right], \\ q_w \;&=\; \frac{1}{3\ A}\left[(h_1 + h_2 + h_3)^2\right] \end{aligned} \tag{12}$$

respectively, where h_i is the edge length from x_{i+1} to x_i. Hence, from equations (8) and (9) the connection between these indicators is that

$$q_m(\underline{h}) = \;\frac{1}{4\ q_b} \;+\; q_w\ \frac{\sqrt{3}}{16}. \tag{13}$$

The choice of norm is not often considered but may be critical in deciding what is the best mesh. Given the linear interpolation error defined by equation (2), Berzins [14] considers the example of Babuska and Aziz [9] in which triangles of the form of that in Figure 2 are used to interpolate the function x^2 with x horizontal. Furthermore Berzins [23] shows that in the L^2 norm the isosceles triangle is more accurate whereas in the H^1 norm right triangles are more accurate and the isosceles triangle is the worst choice as $\alpha \downarrow 0$ in Figure 2. Hence a good mesh in one norm is not necessarily a good mesh in another norm.

The extension to the case of non-quadratic functions may be considered by assuming that the exact solution is locally quadratic and H is thus a local Hessian matrix. Bank [1] uses such an approach inside the code PLTMG and calculates estimates of second derivatives. Adjerid, Babuska and Flaherty [24] use a similar approach based on derivative jumps across edges to estimate the error. An alternative approach is to use the ideas of Hlavacek et al. [25] to estimate nodal derivatives and hence second derivatives.

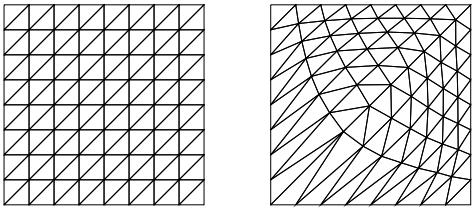

Figure 3: Energy minimisation - original and modified meshes

3 Mesh Movement in 2/3D

The idea that it is important for the the shape of the elements to reflect local solution behaviour, particularly for highly directional flow problems, is well-known [26, 27, 28]. One of the significant steps in realising this understanding was the Moving Finite Element method of Keith Miller, see Baines [29], which continuously moves the mesh for transient problems. Some of the meshes shown by Baines are highly distorted. A similar approach, but rather simpler, was derived by Peraire et al. [30], who applied a simple local iterative procedure based on quantities such as pressure gradients to produce stretched meshes for highly-directional Euler equations flow problems. A key part of their algorithm is a simple Laplacian smoothing approach that has also been used by many others, e.g. Barth [27, 31].

A slightly different approach still is employed by Tourigny and Baines [32], who investigate the construction of locally optimal piecewise polynomial fits to data and produce meshes which vary from smooth to skewed, depending on the solution. The idea is further extended by Tourigny and Hulsemann [33], who minimise an energy functional using a Gauss-Siedel method locally to get similarly skewed meshes. This idea dates back as far as Delfour et al. [34]. Figure 3 shows the original and final meshes for the example used in Section 6.2 of Delfour et al. in which the p.d.e. is given by

$$\frac{\partial^2 u}{\partial x^2} + \frac{\partial^2 u}{\partial y^2} + 56(1 - x - y)^6 = 0 \tag{14}$$

with zero Dirichlet boundary conditions. Rippa and Schiff, [35], present algorithms for constructing minimum energy triangulations by using local operations and also present convincing results to show that these improve the quality of the solution.

Beinert and Kroner [36] move edges so that they are aligned with shock waves and also define a *Blue* direc-

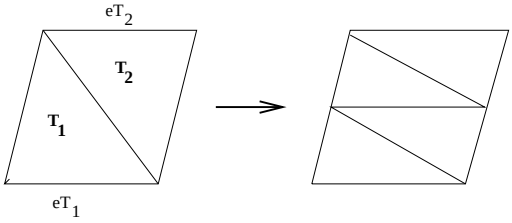

Figure 4: Blue Refinement of Two Triangles into Four.

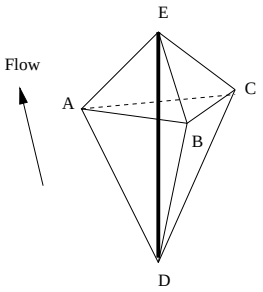

Figure 5: Iliescu's Directional Refinement Procedure.

tional refinement approach. For example in Figure 4 if the edges eT_1, eT_2 are parallel and aligned with the flow direction then the pair of triangles is replaced by four anisotropic triangles. Although the indicator used to guide refinement is the gradient of the Mach number rather than an explicit error estimator, the results are nevertheless impressive.

The relative size of the edge indicators, d_i defined by equation(8) in the previous section gives a means of indicating which edges should be refined to reduce the error. The approach of generating stretched meshes has been used for some time for highly-directional aerospace problems by practitioners such as Mavriplis [37], although the stretching criteria have usually been derived from physical quantities rather than the error directly. One recent method to take advantage of such local gradients is the modified Delaunay approach of Borouchaki et al. [26] in which the local gradient information, of the form of d_i values, is used in conjunction with the Delaunay mesh generator to compute highly stretched grids for anisotropic flows in two space dimensions. The results presented by Borouchaki et al. show that this approach can give good results on problems with highly directional flows. The monograph of George and Borouchaki, [17], uses metrics to define stretched meshes and gives several convincing and realistic examples involving high speed flows regarding the effectiveness of this approach. In addition, a good survey of this type of approach, together with several examples is given by [38].

Other methods using the gradient quantities d_i defined in the previous section are the mesh generation procedure of Simpson [39] and the mesh modification procedure of Ait-Ali-Yahia et al.[40] and Dolejsi [41]. In the latter cases the H matrix is modified to be positive definite by using the absolute values of the eigenvalues. It is not clear that this approach is necessarily valid. Consider for example the function

$$u(x,y) = ax^2 + 2bxy + ay^2, \quad where \quad b > a > 0. \tag{15}$$

The Hessian matrix of this function has eigenvalues $(a-b)$ and $(a+b)$ while the Hessian matrix having eigenvalues $(b-a)$ and $(a+b)$ corresponds to the function

$$v(x,y) = bx^2 + 2axy + by^2. \tag{16}$$

The difference between these functions is only zero when $x = y$ or $a = b$ and otherwise varies greatly over the xy plane, hence casting some doubt on the choice of using the modified Hessian. Ait-Ali-Yahia et al.[40] also use edge indicators, defined in the notation used here by $d_i/\sqrt{\Delta x_i^2 + \Delta y_i^2}$, to move the mesh points. This approach thus scales the edge error component by the edge length. Ait-Ali-Yahia et al. [40] also interpret d_i as the edge length in the H norm.

Mesh redistribution in 3D is less common but Freitag and Ollivier-Gooch [42] and Iliescu [44] give interesting algorithms for splitting tetrahedra. In Iliescu's approach pairs of tetrahedra satisfying convexity and angle conditions related to the flow direction are split into three tetrahedra so as to be aligned with the flow direction, see Figure (5). Freitag and Ollivier-Gooch [42] also provide convincing evidence that mesh smoothing can have beneficial consequences for the rate of convergence of the iterative solver.

A common feature of all the methods listed in this section is that although the mesh is improved in some sense, the criterion used is only indirectly related to the error.

4 Error Estimators with Explicit Geometry Dependence

Recent work in error estimates is starting to reveal the explicit dependence of the error on both solution derivatives and on the mesh. An important stepping stone in this process was the work of Appel, [45, 46], which proved that one can benefit from the presence of small and even large angles of the elements. Appel also shows for bilinear elements that the interpolation and finite element errors coincide. Tsukerman [47, 48]

derives a maximal eigenvalue condition which shows that it is the maximum eigenvalue of the element stiffness matrix that characterises the impact of the shape of the element on the energy norm of the error of the finite element approximation.

Bank and Smith [1], in error analysis for the method used in the PLTMG code, show how the error can be written using d_i and q_b (see Section 2) as a quotient of solution and geometry information:

$$\int_t | \bigtriangledown e_{lin}(x,y)| dx \approx \frac{d_1^2 + d_2^2 + d_3^2}{q_b} \qquad (17)$$

This somewhat simpler form than the expressions in equation(8) and [23] comes about because Bank and Smith consider only the diagonal terms in a matrix to arrive at their approximation. While this error estimator only applies to steady problems, Lang [28] considers transient problems and explicitly includes both solution derivative and geometry information in the error estimates he derives. For 2D reaction-diffusion p.d.e.s modelling highly-directional phenomena such as flame propagation, Lang proves the error estimate:

$$||e_{lin}(x,y)||^2_{H^1} \quad \leq \quad \tilde{c} \left(\sum_{T \epsilon T_k} \eta_T^2 \right)^{1/2} \qquad (18)$$

where the local error estimator $\eta_T^2 = C^2(\tau, \lambda, T)\ D_T^2 U$ and $D_T^2 U$ is a computed approximation to $|u|_2$ as defined by equation (4). The constant $C(\tau, \lambda, T)$ is defined by

$$C(\tau,\lambda,T) = (1 + |\lambda| + \lambda^2)^2 h^2 [0.2587(1 + \frac{1}{\tau})h^2 + \frac{1}{\pi^2}(1 + |\lambda| + \lambda^2)] \qquad (19)$$

and where with reference to Figure 2, $\lambda = tan(\phi)$, h is the longest edge and τ is the timestep. This estimate thus precisely describes the effect of both the geometry and the solution on the error and enables decisions regarding directional refinement to be taken.

The same approach of explicitly defining the relationship between the geometry and the error is also investigated by Barnette [49] in the context of finite difference/volume schemes for simple models of the Navier-Stokes equations. The thesis of Appel [10] considers anisotropic error estimates for singularly perturbed convection-diffusion problems.

5 Linear Tetrahedral Approximation of Quadratics

Although there are now data-dependent tetrahedralisations, see Nielson [15], there are unfortunately very few error estimates for tetrahedral meshes that show the explicit dependence of the error on the mesh and the solution. The natural starting point is perhaps to try and use the interpolation error to assess how appropriate the mesh is for the computed solution. The simple mesh quality indicator of Berzins [19, 23] is based on linear interpolation error estimates and is derived by extending Nadler's [21] approach to tetrahedra by considering the case in which a quadratic function

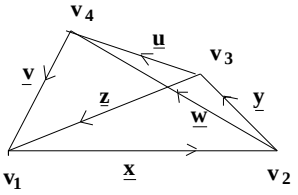

Figure 6: Example Tetrahedron.

$$u(x,y,z) \ = \ \frac{1}{2}\ \underline{x}^T\ H\ \underline{x}\ where \quad \underline{x} \ = \ [x,y,z]^T \quad (20)$$

is approximated by a linear function $u_{lin}(x,y,z)$ defined by linear interpolation based on the values of u at the vertices of a tetrahedron T defined by the vertices v_1, v_2 , v_3 and v_4 as shown in Figure 6.

Let h_i be the length of the edge connecting v_i and v_{i+1} where $v_5 = v_1$. With reference to Figure 6 define the vectors $\underline{\hat{x}}$, $\underline{\hat{y}}$, $\underline{\hat{z}}$, $\underline{\hat{u}}$, $\underline{\hat{v}}$ and $\underline{\hat{w}}$ by $v_2 = v_1 + \underline{\hat{x}}$, $v_3 = v_2 + \underline{\hat{y}}$, $v_1 = v_3 + \underline{\hat{z}} v_4 = v_1 - \underline{\hat{v}}$, $v_4 = v_2 + \underline{\hat{w}}$, $v_4 = v_3 + \underline{\hat{u}}$. Berzins [19] defines the vector of second directional derivatives along edges by

$$\underline{d}^T = \frac{1}{2}\ [d_1, d_2, d_3, d_4, d_5, d_6\ ] \ =$$

$$\frac{1}{2}\left[\underline{\hat{x}}^T H \underline{\hat{x}},\ \underline{\hat{y}}^T H \underline{\hat{y}},\ \underline{\hat{z}}^T H \underline{\hat{z}},\ \underline{\hat{u}}^T H \underline{\hat{u}},\ \underline{\hat{v}}^T H \underline{\hat{v}},\ \underline{\hat{w}}^T H \underline{\hat{w}}\right]$$

and shows that the error may be written in terms of the six directional derivatives along the edges d_i as:

$$\int_T\ (e_{lin}(x,y,z))^2 dx\ dy\ dz = \ \frac{6}{4}\ V\ \frac{8}{7!}\ [(\Sigma d_i)^2 - d_1 d_4 - d_2 d_5 - d_3 d_6 + \Sigma d_i^2\ ]. \quad (21)$$

It is then possible to define the mesh quality indicator in the same way as in Section 2 in that the error is scaled by the maximum directional derivative d_{max}, the integral is scaled by the volume before taking the square root. In a similar way to as in Section 2 define

$$\tilde{Q}(\underline{\tilde{d}}) = \left[(\Sigma \tilde{d}_i)^2 - \tilde{d}_1 \tilde{d}_4 - \tilde{d}_2 \tilde{d}_5 - \tilde{d}_3 \tilde{d}_6 + \Sigma \tilde{d_i}^2\right] \quad (22)$$

Table 1: Interpretation of Q_d Values

Edges Active	1	2	3	4	5	6
$Q_(d)$	2	5-6	9-12	19-22	27-28	39
$Q_(d)/40$	1/20	1/8	1/4	1/2	7/10	1

where $\underline{\tilde{d}} = [\tilde{d}_1, \tilde{d}_2, \tilde{d}_3, \tilde{d}_4, \tilde{d}_5, \tilde{d}_6]^T$. A measure of the anisotropy in the derivative contributions to the error is then provided by Q_{aniso} and a related geometry based indicator by Q_m where

$$Q_{aniso} = \tilde{Q}(\underline{\tilde{d}})/39 \ \ and \ Q_m(\underline{h}) = \frac{C}{V} \ \left[\ \tilde{Q}(\underline{\tilde{h}}) \right]^{\frac{3}{2}} \quad (23)$$

where C is a scaling factor to ensure that the indicator has value one when $h_i = h$. A comparison between this geometry indicator, $Q_m(\underline{h})$, with that of Weatherill Q_w as defined by equation(5) was done by Berzins [19] who showed that the values of the two indicators are very similar. The anisotropic interpolation example used by Berzins, [23], shows that in such circumstances it is important to use indicators such as Q_{aniso} which involve solution information. The indicator $Q_m(\underline{h})$ is related to the mean ratio indicator of Liu and Joe, [18], as defined by η where

$$\frac{1}{\eta^{3/2}} = \frac{C_2}{V} \ \left[(\Sigma h_i^2)^{3/2} \ \right]. \quad (24)$$

where C_2 is a constant, and to the indicator of Weatherill, Q_w defined in equation (6).

Table 1 shows the values of the indicator if 1 to 6 edges are active in that they have equal values of the edge gradients d_i and the remaining edges have zero values of d_i. The variation in the values of Q_d takes into account different permutations of zero and non-zero values of d_i. The table thus provides a way of understanding the meaning of the values produced by the indicator.

6 Laplace's Equation Examples with Finite Element/Volume Tetrahedral Schemes

The issue of mesh suitability for a given solution and numerical solver is recognised as a complex one with no easy answers. There are a variety of views concerning the sensitivity of numerical schemes to distorted meshes. Shephard [50] states that the stabilized FEM for example, appears to have no real problem with elements with angles close to 180 degrees and very large aspect ratios and that tetrahedra with small angles are well-understood to be needed for boundary layer calculations. In contrast, Millar [51, 52], et al. state that for Laplace's equation, finite volume schemes are less sensitive than finite element schemes to sliver-type tetrahedra in meshes. Given the similarity between the finite volume and element schemes in this case, see [27], the difference may be due to implementation issues such as those discussed by Putti and Cordes [53].

In order to understand better the dependency between the mesh and the error, the Laplace equation, $\nabla^2 U = 0$, in three space dimensions of [51] will be used in two simple examples.

6.1 Example 1

In the first case, the mesh of five points consists of a single tetrahedron sub-divided into four by the addition of an internal point and is shown in Figure 7. The analytic solution is given by

$$u(x, y, z) = e^{\pi z} cos(\pi y/\sqrt{2}) sin(\pi(x + 0.5)/\sqrt{2}) \quad (25)$$

where the points O, A, B, C, D and E are defined by:

$$O = [0, 0, 0]^T, \ A = -[0.5, 0.5, 0]^T, \ B = [0.5, -0.5, 0]^T$$

$$C = [0, 1, 0]^T, \ D = [0, 0, 1]^T, \ and \ \ E = [0, 0, \epsilon]^T$$

where ϵ is a parameter that will be varied to test the sensitivity of the numerical solution to the mesh and in particular to distorted elements. The values at A, B, C, D are given by the exact solution and denoted by U_A, U_B, U_C, U_D. The scheme used to approximate the Laplacian is Barth's cell-vertex scheme [27, 31]. This gives a challenging situation for mesh quality indicators as the region associated with each node is composed of parts of all neighbouring tetrahedra. At point E the Laplacian is approximated by

$$\nabla^2 U = W_{EA}(U_A - u_E) + W_{EB}(U_B - u_E) + W_{EC}(U_C - u_E) + W_{ED}(U_D - u_E) \quad (26)$$

where u_E is the numerical approximation to the exact value U_E and is explicitly defined by the equation

$$u_E = (W_{EA}U_A + W_{EB}U_B + W_{EC}U_C + W_{ED}U_D)/ (W_{EA} + W_{EB} + W_{EC} + W_{ED}) \quad (27)$$

In order that the solution satisfies a maximum principle all the weights W_{**} must be positive, [27, 31]. Barth also shows how this condition may not be met on a distorted mesh, but Putti and Cordes [53] show how to modify the method to avoid this and that this also improves the accuracy. This issue is of critical

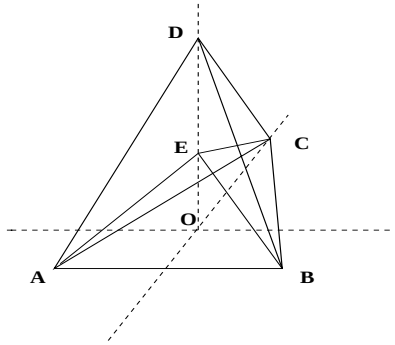

Figure 7: Example Mesh of Four Tetrahedra: ABCE,ABED,ACED and BCED

importance in reacting flow applications such as that outlined in Section 1 because the computation of non-physical negative values will cause the reaction terms to have unphysical values.

Denote the exact solution of the problem at node E by U_E then the p.d.e. truncation error, $TError$, is defined by

$$TError = W_{EA}(U_A - U_E) + W_{EB}(U_B - U_E) + W_{EC}(U_C - U_E) + W_{ED}(U_D - U_E) \quad (28)$$

and the relationship between the truncation error and the error at point E, $Error = U_E - u_E$ is

$$U_E - u_E = -\frac{TError}{(W_{EA} + W_{EB} + W_{EC} + W_{ED})} \quad (29)$$

Table 2 shows the different mesh quality indicators and the interpolation error as the value of ϵ changes for two tetrahedra given by the points ABCE and ACED. The values for the tetrahedra ABED and BCED being similar to those of ACED. With reference to Table 2, Interp is the square of the interpolation error based on the exact solution. In Table 3, Err and T.Err are the error and truncation error defined by equations (29) and (28) respectively. The results in Table 2 show that the anisotropy indicator follows (not surprisingly) the trend of the interpolation error, but that the pointwise discretization error behaves very differently, especially for small values of ϵ. The low values of the anisotropy indicator Q_{aniso} indicate potential problems. The geometry indicator does a good job of picking up the very large error for small ϵ but also erroneously identifies a problem with ϵ close to one, when the error is small.

The interesting result is that both mesh quality indicators do not really identify the relationship between the mesh and the error in the numerical solution. Part of the reason for this is that the volume used by the discretisation method to define the residual at a node is the sum of parts of the volumes of the individual tetrahedra surrounding that node. It is the differing size of the truncation error as caused by the method coefficients that has a dramatic effect on the error. In the case when $\epsilon = 0.001$ the large value of the coefficients W_{ea} and W_{eb}, W_{ec} arise because the face angle between faces such as EBC and ABC is very close to π. Hence in this case the value U_D plays little part in determining u_E. In contrast when ϵ is close to one only one coefficient is large and u_E is determined almost solely by U_D its closest neighbour. The values of the coefficients W_{eb} and W_{ed} etc, are shown in Table 4.

Table 2: Q_{aniso} and Standard Mesh Quality Q_w

	Tet. ABCE			Tet. ACED		
ϵ	Q_{aniso}	Q_w	Interp	Q_{aniso}	Q_{nw}	Interp
0.001	0.35	621	3.4e-6	0.15	2.2	1.0e-3
0.01	0.35	62	3.4e-5	0.15	2.2	1.0e-3
0.5	0.38	1.5	1.6e-3	0.17	3.9	6.2e-4
0.99	0.21	1.1	3.6e-3	0.22	211	2.0e-5
0.999	0.20	1.1	3.6e-3	0.23	211	2.1e-6

Table 3: Solution Error Values

	Numerical Error		
ϵ	U_E	Err	T. Err
0.001	-2.6e-2	0.42	-107.
0.01	-1.7e-2	0.41	-11.4
0.5	5.2e-1	0.01	-0.65
0.99	1.07	3.2e-3	-0.07
0.999	1.08	2.8e-5	-0.06

6.2 Example 2

In the second case consider the simple mesh of 6 tetrahedra used by Barth to demonstrate that a linear tetrahedral finite element solution on a Delaunay mesh may give a solution with the wrong sign. The mesh in Figure 8 is parameterised by the position of node H above G as denoted by Z in the diagram. The

Table 4: Values of the coefficients $W_{ea}, W_{eb}, W_{ec}, W_{ed}$

ϵ	W_{ea}, W_{eb}, W_{ec}	W_{ed}
0.001	8.0e+1	2.52e-1
0.01	9.0	2.72e-1
0.5	8.3e-1	2.5
0.99	7.5e-1	2.2e+2
0.999	7.5e-1	2.4e+3

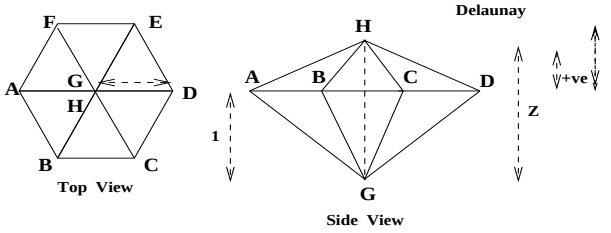

Figure 8: Barth's Example Mesh to demonstrate non-positivity

Table 5: Error Variation with z variation in Barth's Example.

z	E_{Barth}	E_{Putti}	Q_{aniso}	Q_w
0.25	0.07	0.08	0.42	4.3
0.50	0.19	0.25	0.40	2.1
1.00	0.32	0.41	0.34	1.2
1.25	0.22	0.21	0.30	1.1
1.50	0.35	0.01	0.26	1.1
1.80	0.18	0.12	0.31	1.1
2.00	0.29	0.15	0.40	1.2
2.50	0.51	0.06	0.48	1.5
3.00	0.67	3.30	0.40	1.8

coordinates of the mesh points are:

$$A = [-1, 0, 0]^T,\ B = [-0.5, -d, 0]^T,\ C = [0.5, -d, 0]^T$$

$$D = [1, 0, 0]^T,\ E = [0.5, d, 0]^T,\ F = [-0.5, d, 0]^T$$

$$G = [0, 0, -1]^T, and\ \ H = [0, 0, z - 1]^T$$

where z is the parameter being varied and $d = \sqrt{3}/2$. As indicated in Figure 8, Barth shows that the mesh is Delaunay for values of $1 < z < 2$ but gives rise to positive coefficients (see equation(27)) only if $1 < z < 1.75$. In contrast the discretisation of Putti and Cordes [53] gives rise to positive weights for $1 < z < 2$. Hence the mesh quality in this case has a dramatic impact on the quality of the solution. As in Example 1 Laplace's equation is solved for the unknown value at H given Dirichlet conditions at all the other mesh points defined by equation (25). Table 5 shows the errors in the values of u at the point H for different values of z. E_{Barth} is the error using the method described by Barth while E_{Putti} is the error when the method of Putti and Cordes is used. The table shows that the Putti and Cordes method can produce a much more accurate result for some Delaunay meshes, but also for some non-Delaunay meshes that the original method of Barth[27] can give better accuracy sometimes. The anisotropy indicator shows that the amount of anisotropy present is not great while the geometric mesh quality indicator does not, as expected, reflect the error, e.g. for small values of z.

7 Conclusions

The overall conclusion is that the only really satisfactory approach would seem to be to use an error estimator based on both solution and geometry information to modify the mesh. This would appear to be true for strongly directional fluid flows for which highly distorted meshes appear to be very effective. At present, it is still often the case that such estimates which have a clear dependence on both the solution and the mesh for each solution component may not be available or may not be reliable. It is also the case that the availability of such error estimates will always lag behind the problems being solved by practitioners. Hence the mesh generation requirement must be to allow the user to supply mesh quality measures and to choose anisotropic remeshing options. There are, of course, many application areas in which it is still rather difficult to even understand what constitutes a good mesh. One such area is turbulent combustion which may involve the interaction between many chemical species and complex fluid flows. Such problems are like to provide interesting challenges to the meshing community for some time to come. All the evidence suggests that the best meshes in such cases will depend on both the solution and the shape of the mesh elements.

Acknowledgements

The author would like to thank R.Mohammed for providing the meshes shown in Figure 3, the SCI group at the University of Utah for their part of the collaboration that led to Figure 1 and Mark Walkley for his comments on a draft of this paper.

References

[1] Bank, R.E.: Smith, R.K. (1997) Mesh Smoothing Using A Posteriori Error Estimates. SIAM J. Numerical Analysis, 34, 979-997.

[2] Weatherill, N.P.: Marchant, M.J.: Hassan, O. (1993) Unstructured Grid Generation and Adaptation for a transport Aircraft Configuration, Paper presented at 1993 European Forum on Recent

Developments and Applications in Aeronautical Computational Fluid Dynamics. Held at Bristol UK 1-3 September 1993.

[3] Jansen, K.E.,(1999) A stabilized finite element method for computing turbulence. to appear in Computer Methods in Applied Mechanics and Engineering, also see `http://scorec.rpi.edu/~kjansen/`.

[4] Kaltenbach, H-J. (1997) Cell Aspect Ratio Dependence of Anisotropy Measures for Resolved and Subgrid Scale Streses., Journal of Computational Physics 136, 399-410.

[5] Tomlin, A.; Berzins, M.: Ware, J.M.; Smith J.; Pilling, M. (1998) On the use of adaptive gridding methods for modelling chemical transport from multi-scale sources. Atmospheric Env. Vol. 31 (18) 2945-2959.

[6] Johnson, C.R.: Berzins, M., Zhukov, L.; Coffey, R. (1998) SCIRun: Application to Atmospheric Dispersion Problems Using Unstructured Meshes. 111-122 in Numerical Methods for Fluid Dynamics VI (ed. M.J.Baines), ICFD, Wolfson Building, Parks Road, Oxford. ISBN 0 9524929 11.

[7] Zlamal, M. (1968) On the Finite Element Method. Numer. Math. v.12, 394-409.

[8] Strang, G.; Fix G.J. (1973) An Analysis of the Finite Element Method. Prentice Hall Series in Automatic Computation, Englewood Cliffs N.J.

[9] Babuska I.; Aziz, K. (1976) On the Angle Condition in the Finite Element Method., SIAM J. Numer. Anal. 13, 2, 214-226.

[10] Appel, T. (1998) Anisotropic finite element meshes:Local Estimates and Applications. Habilitationschrift. Fakultat fur Mathematik, Technische Universitat Chemnitz-Zwickau, June 1998. (http://www.tu-chemnitz.de/~tap/)

[11] Krizek, M. (1992) On the Maximum Angle Condition for Linear Tetrahedral Elements, SIAM J. Numer. Anal. 29, 2, 513-520.

[12] Shephard, M. (1988) Approaches to the automatic generation and control of finite element meshes., Appl. Mech. Rev. 41,4, 169-185.

[13] Thacker, W.C. (1980) A brief review of techniques for generating irregular computational grids. Int. Jour. for Num. Meths. in Engng. 15, 1980, 1335-1341.

[14] Bern, M.; Epstein, D. (1992) Mesh Generation and Optimal Triangulation. Report CSL 92-1, Xerox Corporation, Palo Alto Research Center, 3333 Coyote Hill Road, Palo Alto, CA 94304.

[15] Nielson, G.M. (1997) Tools for triangulations and Tetrahedralisations and Constructing Functions Defined over Them. Scientific Visualisation - Overviews,Methodologies and Techniques. eds. G.M.Nielson, H.Hagen and H.Muller E.J.Nadler., IEEE Computer Society, Los Alamitos , California, 1997.

[16] Carey, G. (1997) Computational Grids - Generation, Adaptation and Solution Strategies, Taylor and Francis, Bristol PA 19007.

[17] George, P.L.; Borouchaki, H., (1998) Delaunay Triangulation and Meshing- Applications to Finite Elements. Editions Hermes, 8 quai du Marché-Neuf, Paris France, ISBN 2-86601-692-0.

[18] Liu, A.; Joe, B. (1994) Relationship between tetrahedron shape Measures. BIT, 34, 268-287.

[19] Berzins, M. (1998) A Solution-Based Triangular and Tetrahedral Mesh Quality Indicator, SIAM Jour. on Sci. Comput. 19, 2051-2060.

[20] Rippa, S. (1992), Long and thin triangles can be good for linear interpolation. SIAM J. Numer. Anal. 29, 1, pp. 257-270.

[21] Nadler, E.J. (1986), Piecewise linear best l_2 approximation on triangles. in C.K.Chui, L.L.Schumacher and J.D. ward (Eds) Approximation Theory V: Proceedings Fifth International Symposium on Approximation Theory. Academic Press New York, 499-502.

[22] Nadler, E.J. (1985), Piecewise linear approximation on triangulations of a planar region. M.Sc. Thesis, Division of Applied Mathematics, Brown University, Providence, RI.

[23] Berzins, M. (1997) Solution-Based Mesh Quality for Triangular and Tetrahedral Meshes, 427-436 in Proceedings of 6th International Meshing Roundtable, Sandia Report SAND 97-2399, Sandia National Labs, PO Box 5800 MS 0441, Albuquerque, NM 87185-0441.

[24] Adjerid, S.; Babuska, I.; Flaherty, J.E. (1999) A Posteriori Error Estimation for Finite Element Method-of-Lines Solution of Parabolic Problems., Math. Models and Meths. Appl. Sci., (to appear).

[25] Hlavacek, I.; Krizek, M.; Pistora, V. (1996) How to recover the gradient of linear elements on nonuniform triangulations, Applications of Math. 41, 4, 241-267.

[26] Borouchaki, M.; Castro-Diaz, M.J.; George, P.L.; Hecht F.; Mohammadi, B. (1996) Anisotropic adaptive mesh generation in two dimensions for CFD. in Numerical Grid Generation in Computational Field Simulations, (eds) B.K.Soni, J.F. Thompson, J. Hauser, P.Eiseman. Published by NSF Center for Computational Field Simulations , Mississippi State University, Mississippi 39762 USA, ISBN 0-965 1627-02.

[27] Barth, T.J. (1991) Numerical Aspects of Computing Viscous High Reynolds Flows on Unstructured Meshes. AIAA Paper 91-0721, 29th Aerospace Sciences Meeting, January 7-10, 1991, Reno Nevada.

[28] Lang, J. (1995) Two-dimensional fully adaptive solutions of reaction-diffusion equations. Appl. Numer. Math. 18, 223-240.

[29] Baines, M.J. (1994) Moving Finite Elements. Oxford Science Publications.

[30] Peraire, J.; Vahdati, M.; Morgan K.; Zienkiewicz, O.C.(1986), Adaptive Remeshing for Compressible Flow Calculations. J. of Comp. Physics, 22, 131-149.

[31] Barth, T.J. (1994) Aspects of Unstructured Grids and Finite Volume Solvers for the Euler and Navier Stokes Equations. Lecture Notes Presented at the VKI Lecture Series 1994-95.

[32] Tourigny, Y.; Baines, M.J. (1997) Analysis of an Algorithm for Generating Locally Optimal Meshes for L2 Approximation by Discontinuous Piecewise Polynomials. Math. Comp. 66, 218, 623-650.

[33] Tourigny, Y.; Hulsemann, F.(1998) A New Moving Mesh Algorithm for the Finite Element Solution of Variational Problems. SIAM J. Numer. Anal, 35, 4, 1416-1438.

[34] Delfour, M.: Payre, G.; Zolesio, J-P. (1985) An Optimal Triangulation for Second Order Elliptic Problems. Computer Meths. in Applied Mech. and Engnrg, 50, 3, 231-261.

[35] Rippa S.; Schiff, B. (1990) Minimum energy triangulations for elliptic problems. Comput Meths. in Appl. Mech and Engnrg 84, 257-274.

[36] Beinert, R.; Kroner, D. (1993) Finite Volume Methods with Local mesh refinement in 2D, 39-53 in *Adaptive Methods-Algorithms Theory and Applications Numerical Methods for Fluid Dynamics* Volume 46. Proc of 9th Gamm Seminar Kiel January 22-24. Vieweg, Wiesbaden.

[37] Mavriplis, D.M (1990) Adaptive Mesh Generation for Viscous Flows Using Delaunay Triangulation. Jour. of Computational Physics, 90, 271-291.

[38] Buscaglia, C.G.; Dari, E.A. (1997) Anisotropic Mesh Optimisation and its Application in Adaptivity. Int. Jour. for Numer. Meths. in Engng, 40, 4119-4136.

[39] Simpson, R.B. (1994) Anisotropic Mesh Transformations and optimal error control, Appl. Numer. Math., 14, 183-198.

[40] Ait-Ali-Yahia, D.; Habashi, W.G.; Tam, A.; Valet, M-G.; Fortin, M. (1996) A directionally adaptive methodology using an edge based error estimate on quadrilateral grids, Int. Jour. for Num. Meths in Fluids, 23, 673-690.

[41] Dolejsi, V. (1998) Anisotropic mesh adaptation for finite volume and finite element methods on triangular meshes. Computer Visual Sci. 1: 165-178.

[42] Freitag, L.A.; Ollivier-Gooch, C. (1999) A Cost/Benefit Analysis of Simplicial Mesh Improvement Techniques as Measured by Solution Efficiency. To appear in Journal of Computational Geometry and Applications.

[43] Iliescu, T. (1999) A flow-aligning algorithm for convection-dominated problems, Accepted by Int. Jour. Num. Meths. in Engng.

[44] Iliescu, T. (1999) A 3D flow-aligning algorithm for convection-dominated problems, Accepted by Applied Math. Letters.

[45] Appel, T. (1992) Anisotropic interpolation with applications to the finite element method. Computing 47, 277-293.

[46] Appel, T. (1997) Interpolation of non-smooth functions on anisotropic finite element meshes. Preprint SFB393/97-06. Fakultat fur Mathematik, Technische Universitat Chemnitz-Zwickau, (http://www.tu-chemnitz.de/~tap/).

[47] Tsukerman, I. (1998) A General Accuracy Criterion for Finite Element Approximation. IEEE Transactions on Magnetics, 34, 5, September 1998.

[48] Tsukerman, I. (1998) Comparison of Accuracy Criteria for Approximation of Conservative Fields on Tetrahedra. IEEE Transactions on Magnetics, 34, 5, September 1998.

[49] Barnette, D.W. (1998) A Mathematical Basis for Automated Structured Grid Generation with Close Coupling to the Flow Solver. Sandia Report SAND97-2382.

[50] Shephard, M. (1998) *Private communication.*

[51] Millar, G.L.; Talmor, D.; Teng, S. H.; Walkington, N. (1995) A Delaunay Based Numerical Method for Three Dimensions: generation, formulation and partition. 683-692 in Proc 27th ACM Symposium Theory of Computing '95, Las Vegas, USA. ACM Publications, New York.

[52] Millar, G.L.; Talmor, D.; Teng, S. H.; Walkington, N.; Wang, H. (1996) Control Volume Meshes using Sphere Packing- generation, refinement, and coarsening. In the 5th International Meshing Roundtable, 47–61.

[53] Putti M.; Cordes, C. (1998) Finite Element Approximation of the Diffusion Operator on Tetrahedra, SIAM Jour. on Sci. Comput. 19, 1154-1168.